EVS30 Symposium
Stuttgart, Germany, October 9 - 11, 2017

An Improved Thermal Model for Electric Motors

Stefan Oechslen[1], Tobias Engelhardt[1], Axel Heitmann[1], Hans-Christian Reuss[2]

[1]*Dr. Ing. h.c. F. Porsche AG, Porschestraße 911, 71287 Weissach, stefan.oechslen@porsche.de*

[2]*Forschungsinstitut für Kraftfahrwesen und Fahrzeugmotoren Stuttgart (FKFS), Pfaffenwaldring 12, 70569 Stuttgart*

Summary

In high load cycles the components of electric powertrains heat quickly. Overheating can result in irreversible damage. Within the design process, a thermal model to calculate the expected maximum temperatures is essential. To analyze complex, transient operating conditions (e.g. behavior on race tracks), the thermal model is designed as a lumped parameter thermal network (LPTN). The accuracy of LPTNs depend on the number of lumped masses (eq. discretization) and the accuracy of the thermal resistances. Both issues are discussed in this paper as well as recommended methods to determine the thermal conductivity of the winding and to define a sufficient discretization.

Keywords: permanent magnet motor, thermal management, simulation, modeling, cooling

1 Introduction

Due to their high power density and their high level of efficiency, permanent magnet synchronous motors (PMSM) are particularly advantageous as a traction motor in battery-electric sports cars [1]. The low but unavoidable power losses operate like internal heat sources and lead to heating of the motor. Short-term overloads are possible, but cause the component temperatures to quickly rise. As a consequence of persistent high loads, for example when driving on a race track, components can reach critical temperatures. In this case, the power of the motor must be reduced in order to avoid irreversible damage to the motor. The critical components in PMSMs are the windings and the permanent magnets.

Within the scope of design and the development of cooling concepts, a prediction of the expected maximum temperatures is essential. The component temperatures are determined at stationary load points to identify the continuous power. Furthermore, transient load point profiles have to be calculated in order to predict, for example, the available power when driving on a race track. For this purpose, a model with reduced computing time is required. For the development of cooling concepts, it is important that the model is physically based so that new concepts can be easily set up and evaluated. For creating fast computing models, the complexity of the system must be reduced. Thus, modeling investigations are carried out in this paper. The aim is to determine and reduce the influence of the simplifications on the accuracy of the results.

2 Thermal Modeling of Electric Motors

The considered permanent magnet synchronous motor is modeled as a thermal network. In thermal networks, the components are modeled as lumped masses (e.g. [8]). The discretization is relatively coarse compared to a CFD/CHT model. Thus, the computation time can be reduced considerably which allows the analysis of transient load cycles.

The thermal equation of state for a lumped mass (equations (1) and (2)) is derived from the 1st law of thermodynamics [2] as:

$$C_i \cdot \frac{d\vartheta_i}{dt} = P_{L,i} + \sum_j \dot{Q}_{ij} \tag{1}$$

$$\dot{Q}_{ij} = \frac{\vartheta_i - \vartheta_j}{R_{ij}} \tag{2}$$

where t is the time, C_i is the heat capacity, ϑ_i is the temperature and $P_{L,i}$ are the losses of the lumped mass i. $\dot{Q}_{ij}$ is the heat flux and R_{ij} is the thermal resistance between two connected lumped masses i and j.

For a volume element the thermal resistance of heat transfer by heat conduction is given by [2]:

$$R_{cond} = \frac{\Delta x}{\lambda \cdot A} \tag{3}$$

where R_{cond} is the thermal resistance by heat conduction, Δx is the increment of space coordinates, λ is the thermal conductivity and A is the cross-sectional area of the element. Equation (3) shows the importance of thermal conductivity for the accuracy of the model.

The accuracy of thermal networks is discussed in many publications (e.g. [3], [4]). In [4] a detailed investigation to determine a proposed discretization of the considered PMSM is presented. The considered PMSM and the proposed thermal network is shown in Figure 1. The stated investigation concerns the axial and radial discretization of active parts. The proposed thermal model is composed of 8 lumped masses in the axial direction and 4 lumped masses for each active part in the radial direction. This leads to a total number of 151 lumped masses.

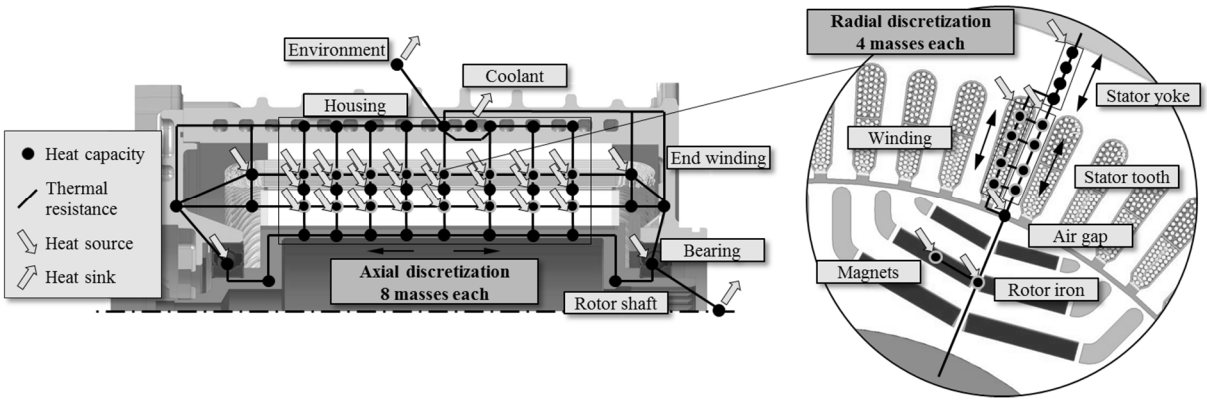

Figure 1: LPTN of the PMSM (axial and radial cut) [4].

3 Important Thermal Conductivities

In this section the thermal conductivities of the important parts of the electric motor are determined. These important parts are the iron sheet stack, the winding and the end windings. The one thing that all of the investigated parts have in common are their anisotropic properties. In addition to known values and measurements, simplified analytical models are presented. A comparison of the available methods show their suitability.

3.1 Thermal Conductivity of the Iron Sheet Stack

The thermal conductivity of the iron sheet stack can be found in data sheets. Furthermore, it can be measured by a TIM tester (TIM: thermal interface material) or by DSC (DSC: differential scanning calorimetry). The measured values, scaled to the values of the data sheet, are shown in Table 1.

Table 1: Thermal conductivity of the iron sheet stack.

	Measurement (TIM tester), scaled to value of data sheet	Measurement (DSC), scaled to value of data sheet
Axial direction	2.42	2.18
Radial / circumferential direction	0.905	1.125

The thermal conductivity in the radial direction of the stack, which is declared in the data sheet, matches the measured values. In the axial direction, the measured thermal conductivity is more than two times greater compared to the data sheet specification. It is worth noting that the thermal conductivity in axial direction depends on the boundary conditions such as the iron sheet coating and the pressing force.

3.2 Thermal Conductivity of the Winding

The thermal conductivity of the winding affects the accuracy of the model. Furthermore, the detected deviation influences the performance of the vehicle significantly, as described, for example, in [5]. A detailed description of the determination of the thermal conductivity of the winding is given in [6].

3.2.1 Thermal Conductivity along the Winding

A modeling approach for calculation of the thermal conductivity of the winding along the conductors is presented in Figure 2.

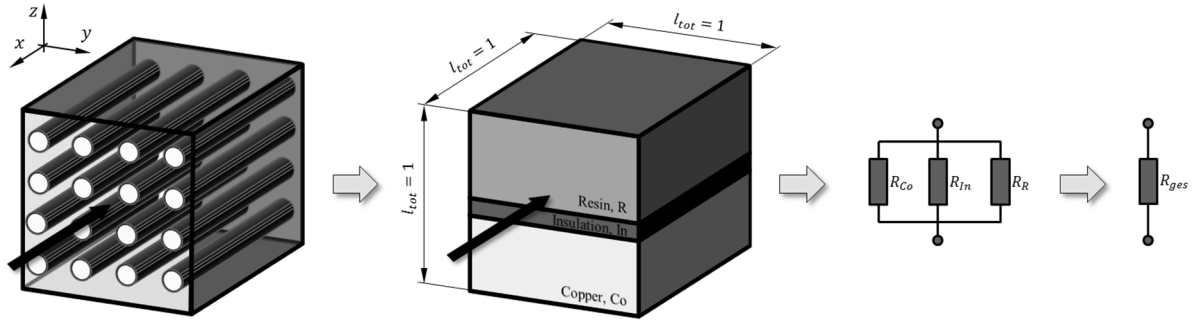

Figure 2: Modeling approach of the thermal conductivity along the winding [6].

The approach to model as a parallel connection leads to equations (4) and (5) for the thermal conductivity [6].

$$f_{Co} = \frac{V_{Co}}{V_{tot}} \quad \text{and} \quad f_{Iso} = \frac{V_{In}}{V_{tot}} \tag{4}$$

$$\lambda_x = \lambda_{Co} \cdot f_{Co} + \lambda_{In} \cdot f_{In} + \lambda_R \cdot (1 - f_{Co} - f_{In}) \tag{5}$$

where f_{Co} and f_{In} are the filling factors of copper and wire insulation calculated from the volumes. λ_{Co}, λ_{In} and λ_R are the thermal conductivities of copper, wire insulation and resin.

3.2.2 Thermal Conductivity across the Winding

For determination of the thermal conductivity across the winding, different methods are available as described in [6]. These are known simplified approaches, measurements, FEM calculations and new approaches. The recommended approach is shown in Figure 3.

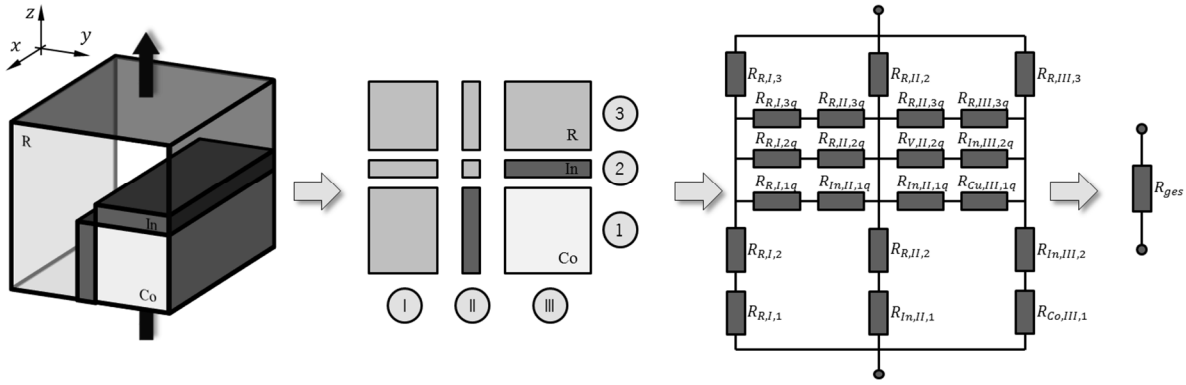

Figure 3: Modeling approach of the thermal conductivity across the winding [6].

In the recommended approach, the geometry is simplified as a square. The thermal resistances of the separate materials are connected as a combination of parallel and serial connections. Thus, the thermal properties can be well represented.

3.3 Thermal Conductivity of the End Windings

The thermal conductivity across the end windings significantly affect the accuracy of the model as well. The thermal conductivity of the end windings can be investigated by a comparison of a maximum detailed LPTN and the measured temperature of the end windings of an electric motor as described in [6]. The absolute temperature deviation is presented in Figure 4. Obviously the thermal conductivity in the axial direction is crucial. In the case of the considered motor the axial thermal conductivity is chosen to be 22 W/(m·K) and the radial thermal conductivity is chosen to be 16 W/(m·K). In this example it is assumed that the measurement error is negligible.

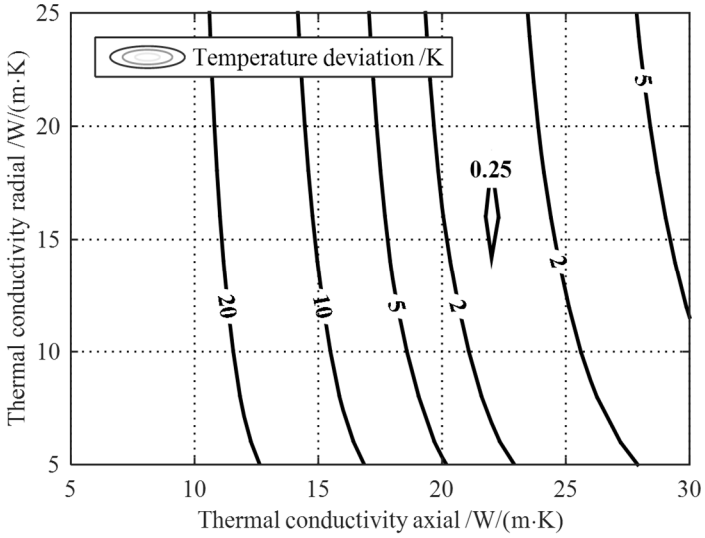

Figure 4: Absolute temperature deviation of maximum end winding temperature of simulation and measurement [6].

Furthermore, in [6] an approach to calculate the thermal conductivities of end windings without measuring data is introduced. In this approach, the thermal conductivity tensor of each end winding is determined as described in 3.2.2. Subsequently, the tensor is rotated by tensor rotation into the middle orientation of the conductors in the particular end winding. This approach leads to similar values.

4 Discretization

In this section the further investigation of the discretization in [4] and the impact on the accuracy of the model is shown. The discretization of the rotor, the end windings, and the winding in the circumferential direction is investigated. Furthermore, the discretization of time and a method to determine a suitable discretization of time and space is shown.

4.1 Discretization of Rotor

In the known thermal model (Figure 1), the rotor is represented by two lumped masses. One represents the magnets and the other one the rotor iron sheet stack. Because of the complex geometry, a more detailed discretization is mentioned. The more extensive model is shown on the right in Figure 5.

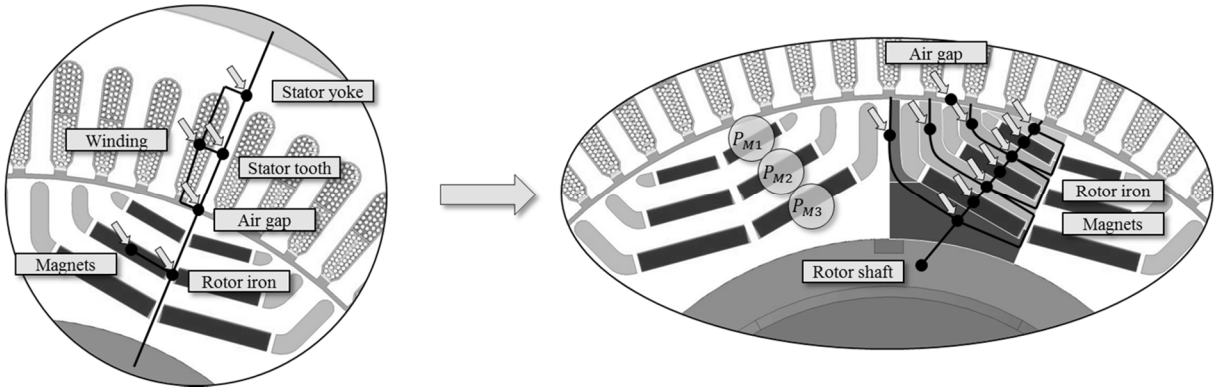

Figure 5: Detailed LPTN of a 3-layer-magnet rotor.

The number of lumped masses for modeling the rotor is increased from two to ten, each multiplied by the number of lumped masses in the axial direction. The magnets are represented by three lumped masses instead of one. One lumped mass is used for each layer of magnets. The rotor iron sheet stack is modelled as seven lumped masses instead of one and is also designed according to the layers. In addition to the advantage of higher temperature resolution, the difference of the permanent magnet losses can be considered in the improved model.

4.2 Discretization of End Windings

In the known thermal model (Figure 1), the end windings are each represented by a single lumped mass. Because of the low thermal conductivity, a higher resolution is proposed. The more extensive model is shown in Figure 6.

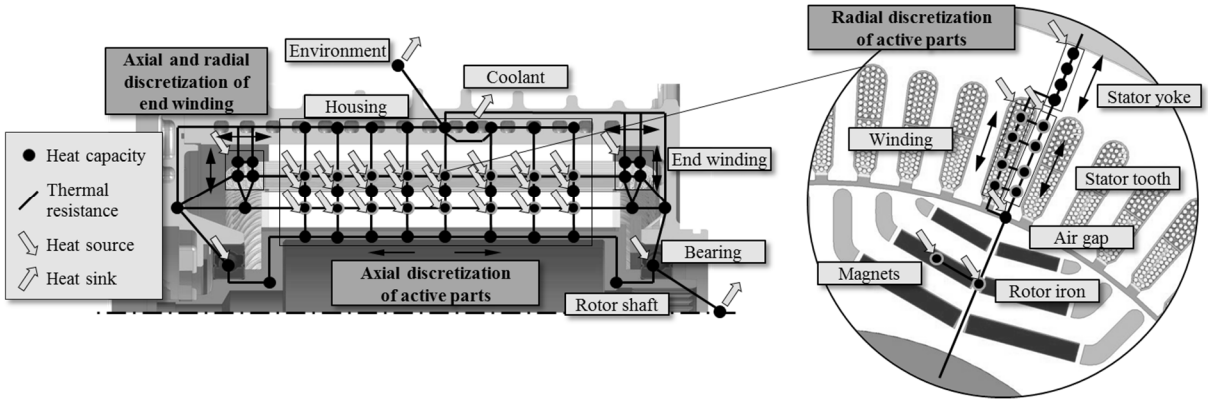

Figure 6: LPTN of the PMSM - Discretization of end windings.

As shown in chapter 3.3 thermal conductivities of the end windings differ in the axial and radial direction. Consequently, the discretization of the end windings can also be varied in the axial and radial direction.

4.3 Discretization of Winding in Circumferential Direction

The windings of the known thermal model (Figure 1) are represented by a single lumped mass in the circumferential direction. Due to the low thermal conductivity, a higher resolution is recommended corresponding to the approach in the radial direction. Figure 7 shows the more extensive model.

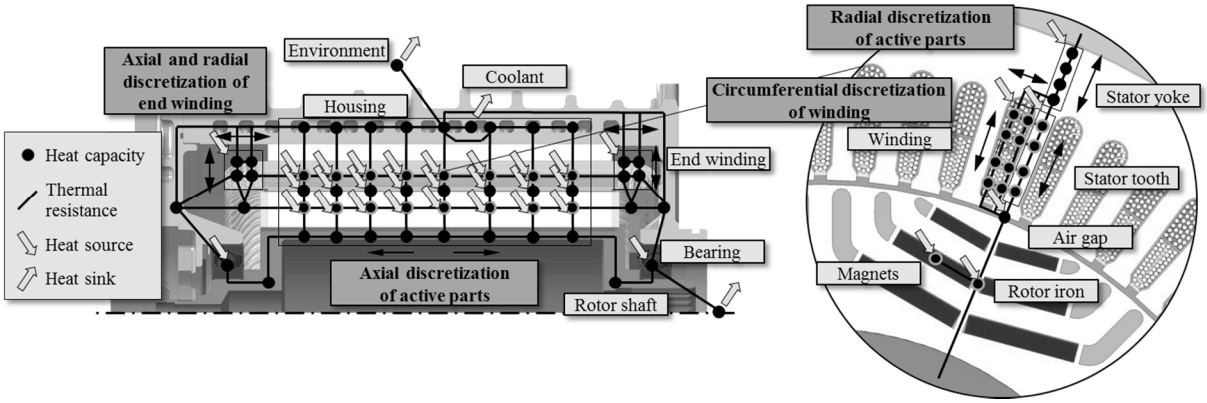

Figure 7: LPTN of the PMSM - Discretization of winding in circumferential direction.

The higher resolution is only applied to the winding. The thermal conductivity of the iron sheet stack of the stator tooth is sufficiently high, so that no higher resolution is required.

4.4 Discretization of Time

In addition to the discretization of space, the discretization of time has a considerable impact on the accuracy of the thermal model.

The flow chart of the thermal simulation is shown in Figure 8. The losses are determined in validated FEM simulations of electromagnetics. In order to reduce the computation time of the thermal simulation, the losses are saved as maps. In the thermal simulation, the losses for each load point are read out from these maps – depending on boundary conditions – and transferred to the thermal model. In the thermal model, the resulting component temperatures are calculated. The insertion of inner iterations extends the approach shown in [4]. As a result, the time step size of the thermal model can be reduced.

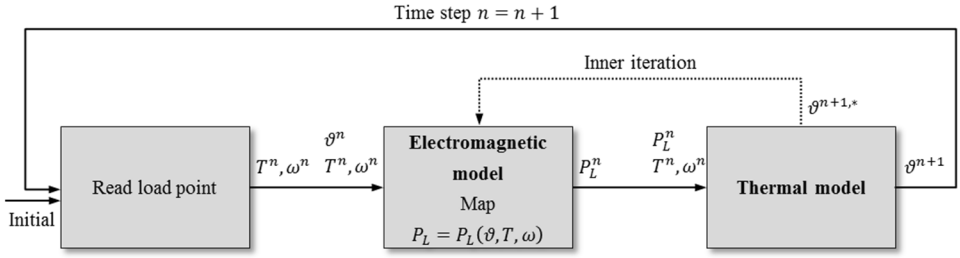

Figure 8: Flow chart of thermal simulation including inner iterations [7].

The discretization of time is of great importance, especially in the case of high resolution of space. This shows the Fourier number defined for problems in the numerical format [2]:

$$Fo = \frac{a \cdot \Delta t}{(\Delta x)^2} \tag{6}$$

where Fo is the Fourier number, a is the thermal diffusivity, Δt is the time step and Δx is the increment of space coordinates.

Stability requirements using the Fourier number are defined, for example, in [2]. These criteria are formulated in such a way that the Fourier number may not exceed a certain value.

4.5 Determination of a Suitable Discretization

As shown above, the model provides six independent ways to modify the discretization of space. These are:

- End windings in axial direction
- End windings in radial direction
- Winding and stator tooth in radial direction
- Stator yoke in radial direction
- Winding in circumferential direction
- Active parts (rotor, magnet, winding, stator tooth, stator yoke), air gap and housing in axial direction

The resulting thermal model is shown in Figure 9.

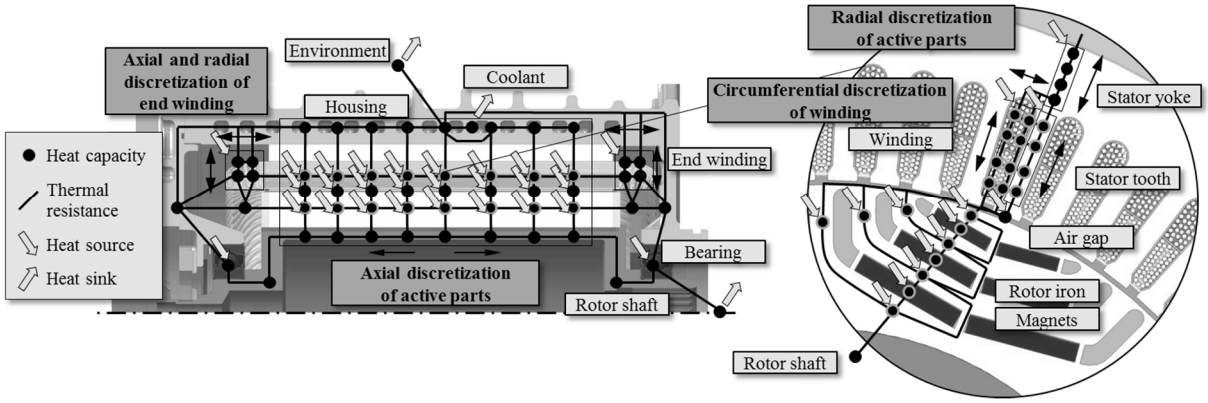

Figure 9: LPTN of the PMSM - Totally discretized.

The calculated maximum temperature of the end windings during a run on a respective race track are shown in Figure 10. The used load cycle corresponds to [4]. With an increasing number of lumped masses and decreasing time step size, the temperatures converge to the discretization independent solution for maximum number of lumped masses and maximum number of inner iterations respectively. A small number of inner iterations correspond to a large time step. It can be seen that this large time step leads to divergence when a high number of lumped masses is used.

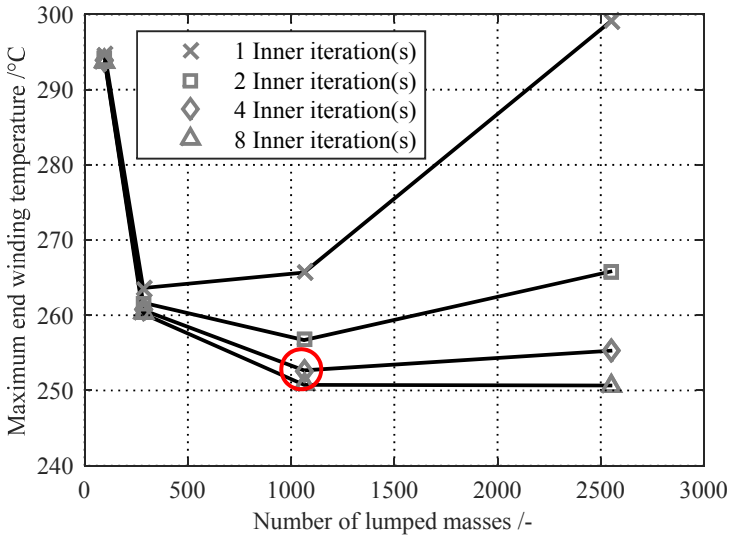

Figure 10: Maximum end winding temperature on a race track over number of lumped masses. Variation of discretization of time and space.

The correlation of the discretization of time and space is of particular importance and can be expressed by equation (7). To solve the LPTN, the approach introduced in [8] is used. Therefore, unstable behavior is not possible. However, as shown, divergent behavior can occur. Therefore, the time step size affects the accuracy and the stability requirement is a useful measure to assess the time step size.

For the thermal resistance and capacity formulation, used for thermal modeling, the stability requirement is (see also [2]):

$$s = \left(\frac{\Delta t}{R_{i,eq} \cdot C_i}\right)_{min} = \left(\frac{\Delta t}{\tau_i}\right)_{min} \leq 1 \tag{7}$$

where s is the stability requirement, Δt is the time step, $R_{i,eq}$ is the thermal equivalent resistance of the lumped mass i, C_i is the thermal capacity of the lumped mass i and τ_i is its thermal time constant.

The values shown in Figure 10 are plotted in Figure 11 over the stability requirement. Because of the use of FTCS-scheme (forward in time, centered in space) the discretization error is squared from the discretization of space and linearly dependent from the discretization of time [9]. These dependencies becomes clear.

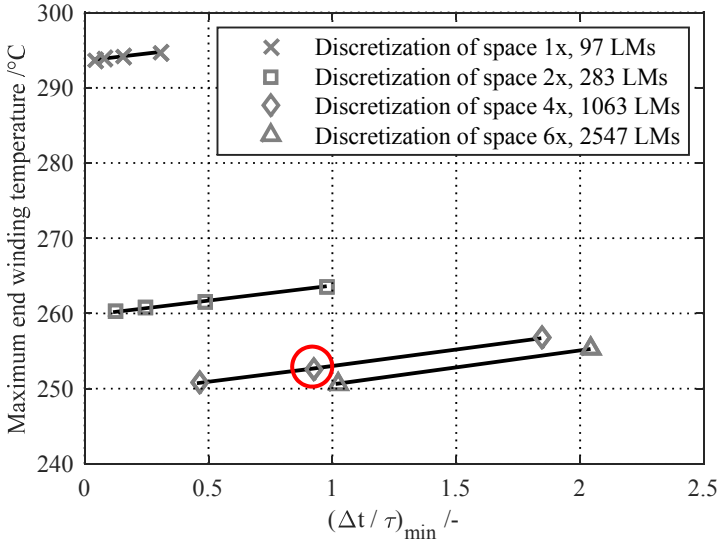

Figure 11: Maximum end winding temperature on a race track over stability requirement (equation (7)). Variation of discretization of time and space. (LM: lumped mass)

When using the mentioned calculation methods, the discretization-independent solution can be found with few supporting points. Theoretically, only two separate discretizations of time and two separate discretizations of space are to be calculated. Four support points are therefore sufficient.

The use of 1063 lumped masses is recommended for the motor shown and its corresponding boundary conditions. The corresponding model is marked in Figure 10 and Figure 11. The resolution is shown in Table 2. This combination provides a deviation of less than 2 K to the discretization independent solution. The stability requirement is less than 1 as proposed in equation (7).

Table 2: Proposed discretization of the LPTN of the considered motor. (LM: lumped mass)

Component	Direction	Value	Unit
Active parts	Axial	8	Number of LMs
End winding (each)	Radial	16	Number of LMs
	Axial	16	Number of LMs
Winding	Circumferential	4	Number of LMs
Stator tooth, winding	Radial	8	Number of LMs
Stator yoke	Radial	8	Number of LMs
Rotor (Iron sheet stack, magnets)	Radial, circumferential	10	Number of LMs
Inner time steps	-	4	Number of steps
Corresponding time step size	-	0,025	s

5 Impact of the Introduced Approaches

This section focuses on the comparison of the presented improvements. In Figure 12 the maximum temperatures of the end windings and magnets when driving on the mentioned race track are shown.

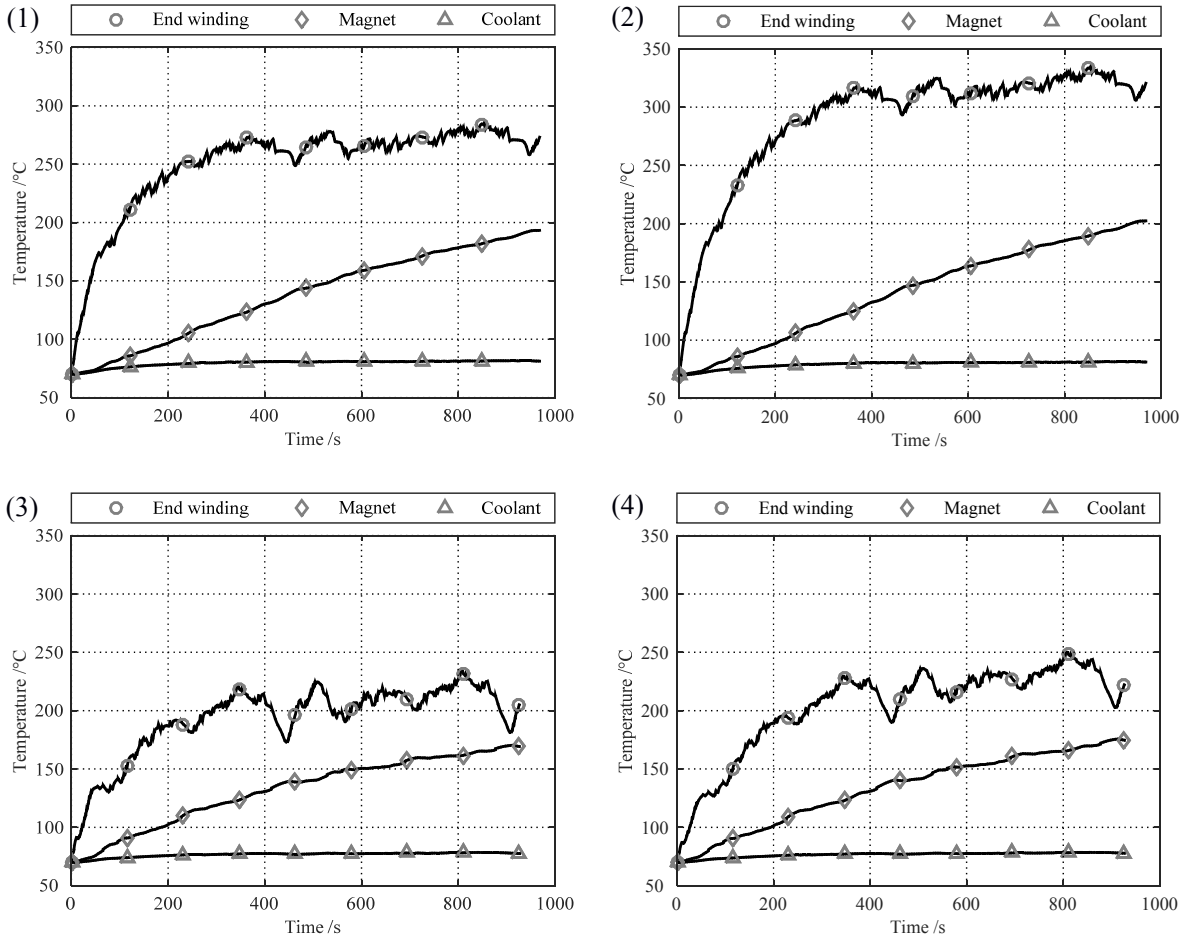

Figure 12: Maximum end winding and maximum magnet temperature on a race track.
(1) Basic discretization, basic thermal conductivities, (2) Basic discretization, new thermal conductivities,
(3) New discretization, basic thermal conductivities, (4) New discretization, new thermal conductivities

The maximum end winding temperature varies significantly as a result of material values and discretization. It can be seen that the new thermal conductivities lead to an increase in the maximum end winding temperature. The new discretization, however, results in a reduction in the maximum end winding temperature. This effect also occurs for the magnet temperature. The magnitude of the temperature deviation is lower, but nevertheless important for the thermal design. The magnitude of the deviation of the new discretization is similar to that of the new thermal conductivities.

The comparison of the basic model (Figure 12, (1)) and the new model (Figure 12, (4)) shows a deviation of 36 K for the end winding temperature and of 15 K for the magnet temperature, which is remarkable.

6 Conclusions

This paper presents improved approaches for LPTNs of electric motors. Approaches to determine thermal conductivities of the winding and the end windings are shown. In the recommended approach, parallel and serial connections of thermal resistances are combined. Thus, the thermal properties can be represented well. The thermal conductivity of the end windings is determined by a comparison of measurements and simulations. For the considered motor, the thermal conductivity is 22 W/(m·K), the radial thermal conductivity is 16 W/(m·K).

Furthermore, a detailed investigation of the discretization of LPTNs is presented. In addition to the known LPTN, the discretization of the end windings, the winding in the circumferential direction, and the rotor is introduced. Another important issue is the discretization of time. Especially in the case of models which show a high discretization of space, the time is also to be finely resolved. Otherwise divergent behavior is to be expected. For this reason, a method to find a suitable discretization (space and time) is presented. This method is applied to the considered motor and a discretization configuration is proposed.

Finally, the impact of the mentioned approaches on the accuracy of the thermal model is determined. It is shown, that both, thermal conductivities and discretization, significantly influence the accuracy.

References

[1] T. Finken, *Fahrzyklusgerechte Auslegung von permanenterregten Synchronmaschinen für Hybrid- und Elektrofahrzeuge*, PhD Thesis, RWTH Aachen, Shaker Verlag, 2011.

[2] J. P. Holman, *Heat Transfer*, Tenth Edition, McGraw Hill, New York, 2010.

[3] G. Dajaku, *Electromagnetic and Thermal Modeling of Highly Utilized PM Machines*, Aachen: Shaker Verlag, 2006.

[4] S. Oechslen, H.-C. Reuss, A. Heitmann, T. Engelhardt, *Thermal Simulation of an Electric Motor in Continuous and Circuit Operation*, 16. Internationales Stuttgarter Symposium, Springer Fachmedien Wiesbaden, 2016.

[5] T. Engelhardt, H.-C. Reuss, A. Heitmann, S. Oechslen, *Analysis of the Effects of High Coil Temperatures on Performance and Drivability of Electric Sports Cars*, 16. Internationales Stuttgarter Symposium, Springer Fachmedien Wiesbaden, 2016.

[6] S. Oechslen, H.-C. Reuss, A. Heitmann, T. Engelhardt, *Thermische Modellierung der Wicklung einer elektrischen Antriebsmaschine*, Tagung: Thermische Auslegung in der Leistungselektronik, Zentrum für Wärmemanagement, Stuttgart, 27.06.2017.

[7] S. Oechslen, *Simulation und Untersuchung des Betriebsverhaltens elektrischer Fahrzeugantriebe unter hoher Belastung*, MSc Thesis, Universität Stuttgart, 2014.

[8] B. Kipp, *Analytische Berechnung thermischer Vorgänge in permanenterregten Synchronmaschinen*, PhD Thesis, Universität der Bundeswehr Hamburg, 2008.

[9] W. Polifke, J. Kopitz, *Wärmeübertragung*, 2. Aktualisierte Auflage, Pearson Studium, 2009.

Authors

Stefan Oechslen was born in 1985 in Ostfildern, Germany. He received the B.Eng. and the M.Sc. degrees in mechanical engineering from the University of Applied Sciences Esslingen, Germany, and from the University of Stuttgart, Germany, in 2012 and 2014, respectively. Since January 2015 he is with the Dr. Ing. h.c. F. Porsche AG, Weissach, Germany, in the department advanced engineering drivetrain and electric drives. His main task is the development of cooling concepts of electric motors. He is simultaneously researching in this field and working towards the Ph.D. degree in cooperation with the University of Stuttgart.

Tobias Engelhardt was born in 1986 in Kitzingen, Germany. From 2006 to 2012, he studied automotive engineering at the University of Stuttgart (Dipl.-Ing.). From 2013 to 2015 he worked for the Research Institute of Automotive Engineering and Vehicle Engines Stuttgart (FKFS). In this time, he participated in a cooperation with the Dr. Ing. h.c. F. Porsche AG which had the aim to develop derating strategies for electric sports cars. Since January 2016, Tobias Engelhardt is working for the Dr. Ing. h.c. F. Porsche AG in the department of advanced engineering for electric powertrains. His main task is the development of powertrain-concepts and electric motors.

Axel Heitmann was born in 1968 in Erlangen, Germany. He received the diploma and Ph.D. degrees in mechanical engineering from the Technical University of Munich in 1993 and 1998, respectively. In 1999, he joined ZF Friedrichshafen AG, Friedrichshafen, Germany, as advanced engineering specialist. From 2004 to 2012, he was with Audi AG, Ingolstadt, Germany, as advanced engineering specialist and project manager. Since 2013, he has been with Dr. Ing. h.c. F. Porsche AG, Weissach, Germany, as manager advanced engineering drivetrain and electric drives.

Hans-Christian Reuss was born in 1959 in Düsseldorf, Germany. He received the Dipl.-Ing. and the Ph.D. degrees in electrical engineering from the Technical University of Berlin, Germany, in 1984 and 1989, respectively. From 1989 to 1993, he was with PHILIPS Semiconductors Application Laboratory in Hamburg, Germany. In 1993 Dr. Reuss became professor at Dresden University of Technology, Dresden, Germany. In 2004 Prof. Reuss moved to Stuttgart to take over the chair of Automotive Mechatronics at the Institute of Internal Combustion Engines and Automotive Engineering (IVK) and to become a member of the management board of the Research Institute of Automotive Engineering and Vehicle Engines Stuttgart (FKFS).